Retina

A Prediction Method of Visual Field Sensitivity Using Fundus Autofluorescence Images in Patients With Retinitis Pigmentosa

Tatsuya Inoue,[1,2] Kosuke Nakajima,[1] Yohei Hashimoto,[1] Shotaro Asano,[1] Kohdai Kitamoto,[1] Kunihiro Azuma,[1] Keiko Azuma,[1] Kazuaki Kadonosono,[2] Ryo Obata,[1] and Ryo Asaoka[1,3,4]

[1]Department of Ophthalmology, The University of Tokyo, Tokyo, Japan
[2]Department of Ophthalmology and Micro-Technology, Yokohama City University, Kanagawa, Japan
[3]Department of Ophthalmology, Seirei Hamamatsu General Hospital, Shizuoka, Hamamatsu, Japan
[4]Seirei Christopher University, Shizuoka, Hamamatsu, Japan

PURPOSE. The purpose of this study was to investigate the association between fundus autofluorescence (FAF) and visual field (VF) sensitivities in eyes with retinitis pigmentosa (RP). We also investigated the model we developed to predict VF sensitivity using the FAF ring and its prediction accuracy.

METHODS. The training dataset consisted of 51 eyes of 28 patients, and the testing dataset consisted of 42 eyes of 25 patients with RP. VF and FAF measurements were conducted using the Humphrey Field Analyzer (HFA) 10-2 test and Optos. The HFA 10-2 test was divided into three sectors according to the association with the FAF (IN, ON, and OUT). Moreover, concentric curves were drawn at 1-degree intervals outside the FAF ring and OUT was divided into six sectors (from OUT1 to OUT6 toward the periphery). Finally, the total deviation (TD) value was predicted using age and visual acuity (VA) in the whole field, and each of the eight sectors was compared.

RESULTS. The TD value decreased significantly from IN, ON, and then toward OUT6. The absolute prediction error with the FAF ring (average, 7.6 dB) was significantly smaller than that without the FAF ring (average, 8.7 dB). The absolute prediction error with the FAF ring was significantly smaller in the central areas (IN, 4.4 dB and ON, 5.3 dB) than those in the peripheral areas (OUT1–6, 6.8–9.1 dB).

CONCLUSIONS. VF sensitivity decreases in association with the FAF ring. We developed a model to predict 10-2 VF sensitivity values using the FAF ring, which enabled us to predict 10-2 TD values.

Keywords: retinitis pigmentosa, fundus autofluorescence, visual field

Retinitis pigmentosa (RP) is a progressive, hereditary retinal disease characterized by nyctalopia and visual field (VF) constriction.[1] Precise measurement of the VF is important in the disease and is usually performed using a static automated perimeter, such as the Humphrey Field Analyzer (HFA; Carl Zeiss Meditec, Dublin, CA, USA).[2,3]

Recent reports have suggested that fundus autofluorescence (FAF) imaging provides an objective measurement of the accumulation of lipofuscin in the retina in various retinal diseases, including age-related macular degeneration, central serous chorioretinopathy,[4,5] and RP.[6,7] In eyes with RP, a characteristic FAF ring is often observed in the macular region, suggesting the accumulation of lipofuscin at the level of the retinal pigment epithelium. Recent studies have suggested that this FAF ring is associated with the deterioration in VF sensitivity. For instance, we have recently indicated that VF sensitivity (measured with an

MP-3 microperimeter; Nidel Co. Ltd., Aichi, Japan) was more closely correlated to the area of the FAF ring than to the area of the disrupted ellipsoid zone measured with optical coherence tomography.[8]

We recently constructed a novel binarization method to automatically identify the FAF ring in eyes with RP (23 eyes) and reported that this method had high intra- and inter-rater agreements.[9] Using this method, we identified the area inside the FAF ring and suggested that this area was significantly correlated with the mean deviation (MD) value with the HFA 10-2 test. In addition, we found that the VF sensitivities decreased significantly from the location inside the FAF ring, toward on, and then outside the FAF ring. The primary purpose of the current study was to revalidate the finding that VF sensitivities decrease in association with the FAF ring (binarization method), using a much larger data set. Based on this result, the secondary purpose of our study
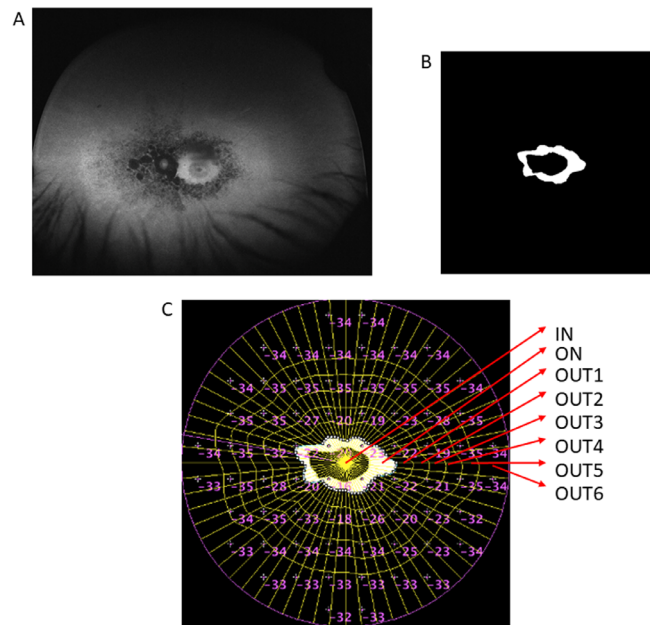
Investigative Ophthalmology & Visual Science

FIGURE 1. Sectorization of the HFA 10-2 test according to the FAF ring. (**A**) Each image output was automatically corrected for 3- to 2-dimensional projection errors. (**B**) The 10 × 10 degrees area was binarized using the Niblack's local thresholding technique. (**C**) Then, the HFA 10-2 test was superimposed and sectorized according to the FAF ring. FAF, fluorescence autofluorescence; HFA, Humphrey Field Analyzer; IN: inside the FAF ring (IN), ON: on the FAF ring (ON), OUT1: between the FAF outer ring and 1 degree outside the FAF outer ring, OUT2: between 1 and 2 degrees outside the FAF outer ring, OUT3: between 2 and 3 degrees outside the FAF outer ring, OUT4: between 3 and 4 degrees outside the FAF outer ring, OUT5: between 4 and 5 degrees outside the FAF outer ring, and OUT6: 5 degrees or more outside the FAF outer ring.

was to develop a model to predict the results of HFA 10-2 test using the FAF ring (binarization method) and to investigate its accuracy.

METHODS

This retrospective cross-sectional study was approved by the Research Ethics Committee of the Graduate School of Medicine and the Faculty of Medicine of the University of Tokyo. Patients with RP agreed to the storage and use of their information in the database and their written informed consent was obtained. This study was performed according to the tenets of the Declaration of Helsinki.

Patients

The present study enrolled 93 eyes of 53 consecutive patients with RP who presented with the FAF ring within 10 degrees at the macula. All patients fulfilled the following inclusion criteria: (1) typical fundus findings of RP, such as bone spicule pigmentation, arteriolar attenuation, and waxy disc pallor; (2) reduction in a- and b-wave amplitudes or nondetectable full-field electroretinogram; (3) RP was the only disease causing VF damage; and (4) both HFA and wide-field FAF imaging were measured within 3 months. The best corrected visual acuity (BCVA) was measured as a decimal visual acuity (VA) using the Landort C chart and was converted to the logarithm of the minimum angle of resolution (logMAR) VA. Eyes with apparent cataract demonstrating suboptimal FAF images were excluded and eyes with macular edema on the optical coherence tomography (OCT) images were also excluded.

VF Testing

An HFA 10-2 measurement was performed with the Swedish Interactive Threshold Algorithm Standard testing algorithm. Only reliable VFs, which were defined as a fixation loss rate < 20% and a false-positive rate < 15%, were used in the analyses by following the criteria used by the HFA software. The false-negative rate was not used as an exclusion criterion.[10]

FAF Imaging

The FAF image was obtained without pupil dilation using an ultra-widefield imaging system (Optos 200Tx; Optos, Dunfermline, Scotland, UK), which uses a 532-nm exciter filter and a 570 to 780-nm barrier filter for autofluorescence (AF) detection. This instrument allows a 200-degree visualization of the retina in a single frame. Images with eyelash interference were excluded, as were those in which the macula was largely shifted from the center.

FAF Image Processing

FAF image processing was performed using the algorithm described previously.[9] Briefly, each image output (Fig. 1A) was automatically corrected for 3- to 2-dimensional projection errors by the V2 Vantage Pro software (Optos). They were processed using Fiji software version 1.0, based on ImageJ (version 1.47, http://imagej.nih.gov/ij/; National Institutes of Health, Bethesda, MD, USA). The locations of the fovea and disc were then decided manually and Niblack's local thresholding technique was performed to binarize each image (Fig. 1B).[11,12]

FIGURE 2. Examples of discontinuous and irregular-shaped AF rings. A discontinuous FAF ring was observed in four eyes (**A**) and an irregular-shaped FAF ring was seen in 12 eyes (**B**). These eyes were excluded from the current analysis. BCVA, best corrected visual acuity; FAF, fluorescence autofluorescence.

A total of 64 half lines were drawn every $\pi/32$ radian starting from the fovea. Two intersection points were identified in each line, with one at the inner border of the FAF ring and the other at the outer border of the FAF ring. The distance between these two intersection points was defined as the ring width, and the distance between the fovea and inner intersection was defined as the inner radius. In addition, the area inside FAF and the area on the FAF ring were calculated automatically.

The image was first divided into the following three sectors: inside the FAF ring (IN), on the FAF ring (ON), and outside the FAF ring (OUT). Moreover, concentric curves were drawn at 1-degree intervals outside the FAF ring. The image was then divided into eight sectors according to the relationship with the FAF ring; inside the FAF inner ring (IN), on the FAF ring (ON), between the FAF outer ring and 1 degree outside the FAF outer ring (OUT1), between 1 and 2 degrees outside the FAF outer ring (OUT2), between 2 and 3 degrees outside the FAF outer ring (OUT3), between 3 and 4 degrees outside the AF outer ring (OUT4), between 4 and 5 degrees outside the FAF outer ring (OUT5), and 5 degrees or more outside the FAF outer ring (OUT6). Finally, the total deviation (TD) of the HFA 10-2 test was superimposed (Fig. 1C) and sectorized.

Among the 93 eyes, some eyes demonstrated a discontinuous FAF ring (Fig. 2A) and others demonstrated continuous but irregular-shaped FAF rings (Fig. 2B). The discontinuous FAF was observed in 4 eyes and the irregular-shaped AF ring in 12 eyes. These eyes were not included in the current study. All judgments were performed by two independent ophthalmologists (T.I. and K.N.). When the judgments did not agree between the two investigators, they discussed the inclusion criteria again.

Training and Testing Datasets

The training dataset consisted of 51 eyes of 28 patients with RP. All 23 eyes analyzed in our previous study[9] were included in this group (28 eyes were newly collected). After this dataset was created, additional data were collected from 42 eyes of 25 patients with RP and used as the test dataset.

Prediction of VF Using AF

Without the AF Ring (Binarization Method). Using the training dataset, a multivariate linear regression model was constructed between the TD values at each test point in the HFA 10-2 test and the values of age and logMAR VA. Using this model, 68 TD values in the testing dataset were predicted, and the absolute prediction error was calculated as the absolute difference between the predicted and actual TD values.

With the AF Ring (Binarization Method). A multivariate linear regression model was constructed to predict the TD values from the values of age and logMAR VA, and the areas of IN and ON, using the training dataset. This was conducted in each of the eight sectors separately, so that each parameter could have a different (optimal) coefficient value at each sector. Then, using this model, 68 TD values in the testing dataset were predicted, and the absolute prediction error was calculated.

Statistical Analysis

The absolute prediction errors to predict 68 TD values in the HFA 10-2 test were compared between the methods with and without the FAF ring (binarization method), using the linear mixed model, whereby subjects were treated as random effects. The linear mixed model is equivalent to ordinary linear regression in that the model describes the relationship between the predictor variables and a single outcome variable. However, standard linear regression analysis assumes that all observations are independent of each other. In the current study, measurements were nested within subjects, and, hence, were dependent on each other. Ignoring this grouping of the measurements will result in the underestimation of standard errors of regression coefficients. The linear mixed model adjusts for the hierarchical structure of the data, modeling in a way in which measurements are grouped within subjects to reduce the possible bias derived from the nested structure of data.[13,14]

The absolute prediction errors to predict 68 TD values in the HFA 10-2 test with the FAF ring (binarization method) were compared across the sectors, using the linear mixed model and Tukey's test. In addition, the associations between the absolute prediction error and the values of logMAR VA and TD were analyzed using the linear mixed model. All analyses were performed using the statistical programming language R (R version 3.3.3; R Project for Statistical Computing, Vienna, Austria).

RESULTS

Table 1 shows the demographic characteristics of the training and test datasets. The mean age ($\pm$ standard deviation [SD]) was 45.1 ± 18.0 and 52.9 ± 18.3 years in the training and test datasets, respectively. The mean logMAR VA was 0.18 ± 0.32 and 0.31 ± 0.46 in the training and test datasets, respectively.

In the training dataset, foveal sensitivity was significantly correlated with the logMAR VA ($P < 0.001$, linear mixed model); the logMAR VA was $1.88–0.051$ (± 0.0053) $\times$ foveal sensitivity (Fig. 3A). The MD value was also related to the logMAR VA ($P = 0.002$, linear mixed model); the logMAR VA was $-0.012–0.017$ (± 0.0055) $\times$ MD (Fig. 3B).

The comparison of the TD values in each sector (IN, ON, OUT1, OUT2, OUT3, OUT4, OUT5, and OUT6) in all 93 eyes is shown in a boxplot (Fig. 4) and Table 2. There was a significant difference in all comparisons across the sectors ($P < 0.05$, Tukey's test and linear mixed model); the TD values decreased significantly from IN toward OUT6.

TABLE 1. Demographic Characteristics of the Training and Testing Datasets

Variables	Training Dataset	Testing Dataset
Eyes, R/L	18/17	20/22
Sex, F/M	12/13	10/15
Age, mean ± SD, y	45.1 ± 18.0	52.9 ± 18.3
LogMAR VA, mean ± SD, mm	0.18 ± 0.32	0.31 ± 0.46
MD of HFA 10-2 test, mean ± SD, dB	−15.8 ± 7.9	−18.6 ± 9.9

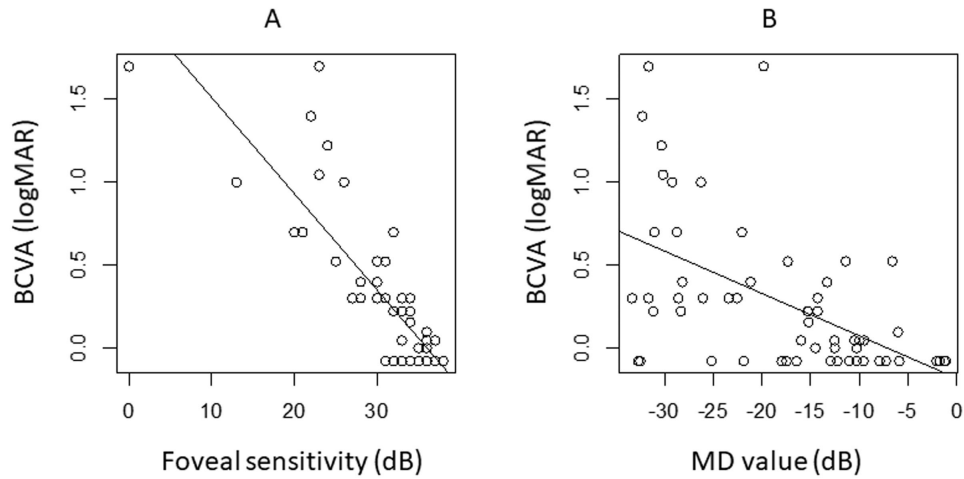SD, standard deviation; VA, visual acuity; MD, mean deviation; HFA, Humphrey Field Analyzer.

FIGURE 3. The relationship between VF sensitivity and the logMAR VA. There was a significant association between foveal sensitivity and the logMAR VA (**A**). A significant relationship was also observed between the MD value and the logMAR VA (**B**). VF, visual field; MD, mean deviation; VA, visual acuity.
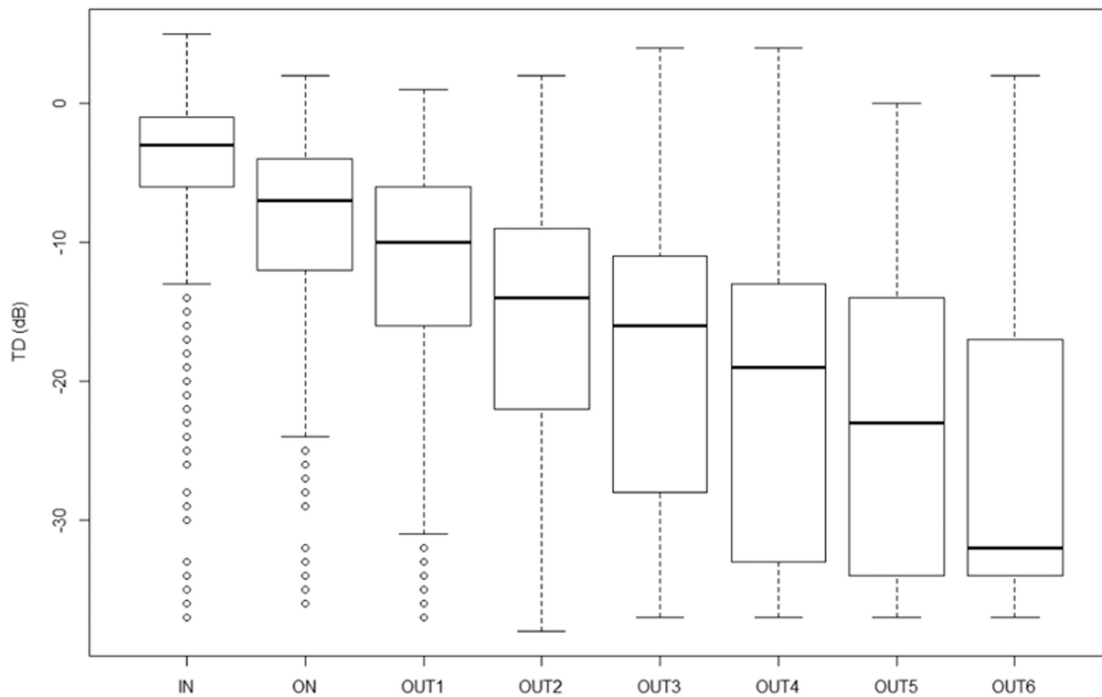

FIGURE 4. The comparison of the TD values in each sector. There was a significant difference in all the comparisons across the sectors ($P < 0.05$, Tukey's test and linear mixed model). FAF, fluorescence autofluorescence; IN, inside the FAF ring; ON, on the FAF ring; OUT1, between the FAF outer ring and 1 degree outside the FAF outer ring; OUT2, between 1 and 2 degrees outside the FAF outer ring; OUT3, between 2 and 3 degrees outside the FAF outer ring; OUT4, between 3 and 4 degrees outside the FAF outer ring; OUT5, between 4 and 5 degrees outside the FAF outer ring; OUT6, 5 degrees or more outside the FAF outer ring; TD, total deviation.

TABLE 2. TD Values in Each Sector

Sector	Mean	SD	P Value (vs. IN)	P Value (vs. ON)	P Value (vs. OUT1)	P Value (vs. OUT2)	P Value (vs. OUT3)	P Value (vs. OUT4)	P Value (vs. OUT5)
IN, dB	−4.8	6.6	–	–	–	–	–	–	–
ON, dB	−8.5	7.2	**<0.001**	–	–	–	–	–	–
OUT1, dB	−11.6	8.4	**<0.001**	**<0.001**	–	–	–	–	–
OUT2, dB	−15.9	9.7	**<0.001**	**<0.001**	**<0.001**	–	–	–	–
OUT3, dB	−18.3	10.4	**<0.001**	**<0.001**	**<0.001**	**<0.001**	–	–	–
OUT4, dB	−20.6	10.6	**<0.001**	**<0.001**	**<0.001**	**<0.001**	**0.016**	–	–
OUT5, dB	−23.0	10.5	**<0.001**	**<0.001**	**<0.001**	**<0.001**	**<0.001**	**0.0027**	–
OUT6, dB	−26.0	10.0	**<0.001**	**<0.001**	**<0.001**	**<0.001**	**<0.001**	**<0.001**	**0.042**

P values in bold suggest *P* < 0.05.
TD, total deviation; IN, inside the FAF ring (IN); ON, on the FAF ring (ON); OUT1, between the FAF outer ring and 1 degree outside the FAF outer ring; OUT2, between 1 and 2 degrees outside the FAF outer ring; OUT3, between 2 and 3 degrees outside the FAF outer ring; OUT4, between 3 and 4 degrees outside the FAF outer ring; OUT5, between 4 and 5 degrees outside the FAF outer ring; OUT6, 5 degrees or more outside the FAF outer ring; FAF, fluorescence autofluorescence.

TABLE 3. Absolute Prediction Error Values with AF Ring (Binarization Method) Across Eight Sectors

Sector	Mean	SD	P Value (vs. IN)	P Value (vs. ON)	P Value (vs. OUT1)	P Value (vs. OUT2)	P Value (vs. OUT3)	P Value (vs. OUT4)	P Value (vs. OUT5)
IN, dB	4.4	4.7	–	–	–	–	–	–	–
ON, dB	5.3	5.0	0.22	–	–	–	–	–	–
OUT1, dB	6.8	4.8	**<0.001**	**<0.001**	–	–	–	–	–
OUT2, dB	8.3	5.0	**<0.001**	**<0.001**	**0.011**	–	–	–	–
OUT3, dB	8.9	5.0	**<0.001**	**<0.001**	**<0.001**	0.23	–	–	–
OUT4, dB	9.1	5.8	**<0.001**	**<0.001**	**<0.001**	0.12	1.00	–	–
OUT5, dB	8.8	5.7	**<0.001**	**<0.001**	**<0.001**	0.54	**<0.001**	0.996	–
OUT6, dB	7.6	5.7	**<0.001**	**<0.001**	0.097	0.95	1.00	**<0.001**	**0.016**

P values in bold suggest *P* < 0.05.
IN, inside the FAF ring (IN); ON, on the FAF ring (ON); OUT1, between the FAF outer ring and 1 degree outside the FAF outer ring; OUT2, between 1 and 2 degrees outside the FAF outer ring; OUT3, between 2 and 3 degrees outside the FAF outer ring; OUT4, between 3 and 4 degrees outside the FAF outer ring; OUT5, between 4 and 5 degrees outside the FAF outer ring; OUT6, 5 degrees or more outside the FAF outer ring; FAF, fluorescence autofluorescence.

In the training dataset, 405, 328, 365, 398, 458, 464, 411, and 639 test points were assigned to the regions of IN, ON, OUT1, OUT2, OUT3, OUT4, OUT5, and OUT6, respectively. These values were 273, 247, 262, 326, 348, 371, 333, and 696, respectively, in the testing dataset. With the training dataset, at each sector, the association between the TD values from the values of age, logMAR VA, and the areas of IN and ON was as follows:

IN: $-9.1 - 0.021 \times$ age $-7.1 \times$ logMAR VA $+ 3.2 \times 10^{-5} \times$ IN area $+ 1.7 \times 10^{-4} \times$ ON area

ON: $-10.3 - 0.031 \times$ age $-5.5 \times$ logMAR VA $- 7.5 \times 10^{-6} \times$ IN area $+ 1.8 \times 10^{-4} \times$ ON area

OUT1: $-10.5 - 0.046 \times$ age $-6.1 \times$ logMAR VA $+ 1.1 \times 10^{-4} \times$ IN area $+ 1.1 \times 10^{-4} \times$ ON area

OUT2: $-10.9 - 0.059 \times$ age $-2.5 \times$ logMAR VA $+ 2.0 \times 10^{-4} \times$ IN area $+ 2.4 \times 10^{-5} \times$ ON area

OUT3: $-20.2 - 0.029 \times$ age $-4.5 \times$ logMAR VA $+ 2.8 \times 10^{-4} \times$ IN area $-2.0 \times 10^{-5} \times$ ON area

OUT4: $-27.7 - 0.0049 \times$ age $-6.5 \times$ logMAR VA $+ 3.3 \times 10^{-4} \times$ IN area $+ 1.2 \times 10^{-4} \times$ ON area

OUT5: $-24.2 - 0.022 \times$ age $-4.3 \times$ logMAR VA $+ 5.3 \times 10^{-4} \times$ IN area $-3.5 \times 10^{-4} \times$ ON area

OUT6: $-27.1 - 0.025 \times$ age $-2.4 \times$ logMAR VA $+ 5.2 \times 10^{-4} \times$ IN area $-2.5 \times 10^{-4} \times$ ON area

The comparison between the absolute prediction error with (7.6 ± 5.6 dB) and without (8.7 ± 15.4 dB) the FAF ring (binarization method) is shown in Figure 5. There was a significant difference between the two values ($P < 0.001$, linear mixed model).

The comparison of the absolute prediction error values with the FAF ring (binarization method) prediction across the eight sectors is shown in Figure 6 and Table 3. The IN and ON values were significantly smaller than those at all the six OUT sectors ($P < 0.05$, Tukey's test and linear mixed model). The values of OUT1 were significantly smaller than those of OUT2, OUT3, OUT4, and OUT5 ($P < 0.05$).

Among the 68 test points from 41 eyes (2788 test points), there were 95 test points, which had the absolute prediction error > 20 dB. These test points distributed wide in each area 2.2% in IN (6 test points), 3.2% in ON (8), 2.3% in OUT1 (6), 3.1% in OUT2 (10), 3.4% in OUT3 (12), 4.0% in OUT4 (15), 4.2% in OUT5 (14), and 3.4% in OUT6 (24). There were 10 eyes that had at least one test point with the absolute prediction error > 20 dB. Among these, there were 3 eyes with > 10 such test points (30 test points in 2 eyes and 12 test points in 1 eye). Analyzing the accompanied OCT images of these eyes, it was suggested that the ellipsoid zone was disrupted in the IN area and remained in the OUT areas in these eyes (see a typical case in Fig. 7). The remaining 7 eyes had 3.3 ± 2.4 (range: from 1 to 8) test points with the absolute prediction error > 20 dB, otherwise nil; such finding was not observed in these eyes.

There was a significant association between absolute prediction error and the values of logMAR VA (coefficient = -2.00, standard error = 0.94, $P = 0.039$, linear
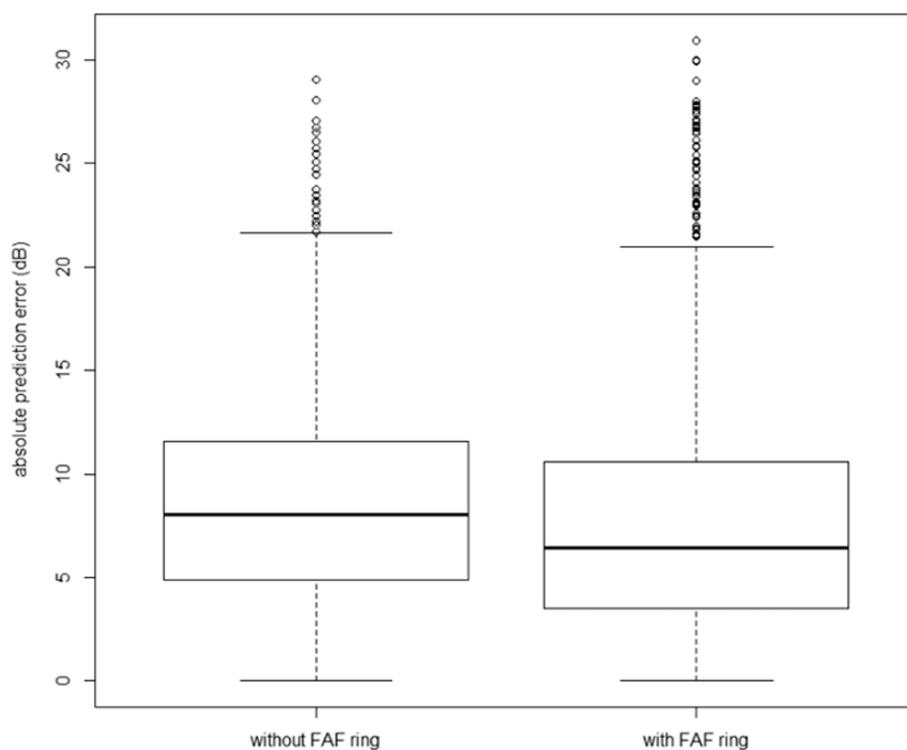
Figure 5. The comparison between the absolute prediction error with (7.6 ± 5.6 dB) and without (8.7 ± 15.4 dB) the FAF ring. There was a significant difference between the two values. FAF, fluorescence autofluorescence.

mixed model) and also TD value at each point (coefficient = −0.093, standard error = 0.011, P <0.001), suggesting that the absolute prediction error increased with the deterioration of these visual functions.

DISCUSSION

In the present study, FAF ring identification using the binarization method was conducted in eyes with RP, along with the HFA 10-2 test. The VF sensitivity (TD value) was calculated at each sector. As a result, it was suggested that the value decreased from within the FAF ring, toward on, and then outside the FAF ring (from OUT1 to OUT6), similar to the results of our previous study.[9] In addition, the TD value was predicted using age and the logMAR VA in the whole field. We investigated whether this prediction could be improved by conducting the prediction in each FAF sector separately. As a result, we found that it was significantly useful to use the FAF ring sector when predicting the HFA 10-2 test. In addition, FAF measurements without pupil dilation are easy to examine and comfortable, so it is clinically effective, if VF is predicted accurately from FAF like in the currently proposed method.

In our previous study,[9] the HFA 10-2 test was similarly subdivided according to the relation to the FAF ring, however no significant differences were observed between OUT3 and OUT4, OUT4 and OUT5, OUT5 and OUT6. Preparing a larger number of eyes in the current study, the TD value was significantly different across all of the eight sectors, which implies that the binarization method was a valid approach (Fig. 4 and Table 2). This motivated us to predict

the TD values using the FAF ring, as well as age and BCVA. Consequently, the current study suggested that a significantly more accurate prediction was achieved when the FAF ring was used, compared with that when only age and VA were used (Fig. 5).

The absolute prediction errors of the TD values were small, especially in IN and ON (Fig. 6 and Table 3). This may be because the BCVA is more closely related to the VF sensitivities in the central area than those in the more peripheral areas. A previous study suggested that the BCVA was closely correlated with VF sensitivities in the central area, but not with those in the peripheral area, in eyes with glaucoma.[15] Indeed, in the formulas of predicting the TD values, the coefficient values of VA were larger than those in the outer sectors. In contrast to the small absolute prediction error in the central areas, the prediction accuracy was much higher in the more peripheral areas, even with the FAF ring method (binarization method). Another reason for the tighter prediction errors in these regions may be the relatively narrower variation of the TD values (Table 2). Further efforts are still needed to improve the prediction accuracy in this region, such as by considering the information of the outer segment layer.

Sayo et al. have suggested that the thickness of the outer segment was strongly correlated with the VF sensitivity in eyes with RP, agreeing with the pathology of the disease.[16] The Optos imaging system is a noninvasive and nonmydriatic measurement instrument. Recent advances now allow for the FAF to be easily observed in patients with RP in the clinical setting. Recent studies have suggested the advantage of using this measurement in eyes with RP. Oishi et al.
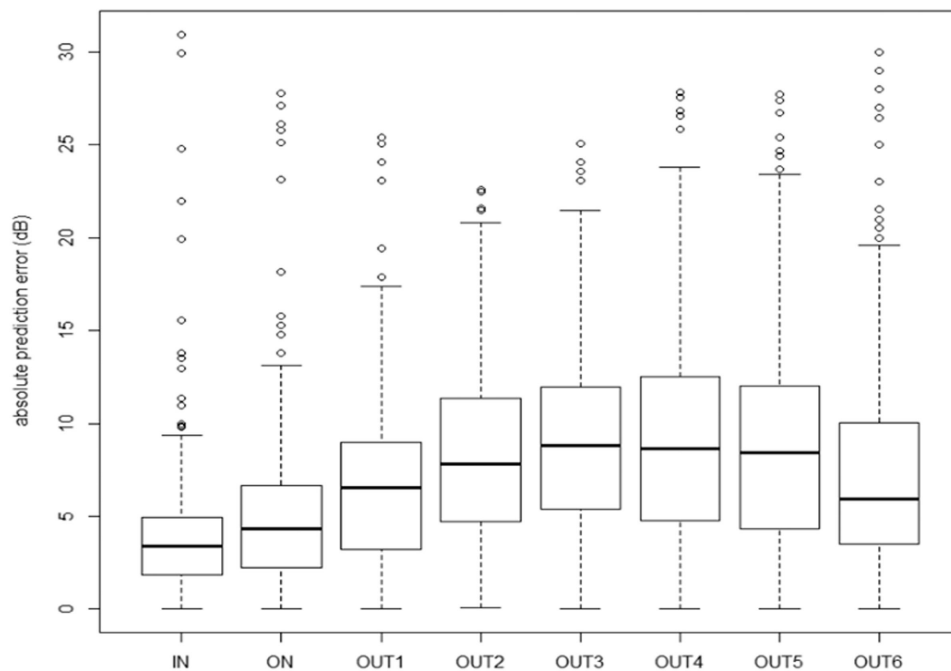
Figure 6. Absolute prediction error values with the FAF ring (binarization method) prediction across eight sectors. The IN and ON values were significantly smaller than those at all six OUT sectors. The values of OUT1 was significantly smaller than those of OUT2, OUT3, OUT4, and OUT5. FAF, fluorescence autofluorescence; IN, inside the FAF ring; ON, on the FAF ring; OUT1, between the FAF outer ring and 1 degree outside the FAF outer ring; OUT2, between 1 and 2 degrees outside the FAF outer ring; OUT3, between 2 and 3 degrees outside the FAF outer ring; OUT4, between 3 and 4 degrees outside the FAF outer ring; OUT5, between 4 and 5 degrees outside the FAF outer ring; OUT6, 5 degrees or more outside the FAF outer ring.
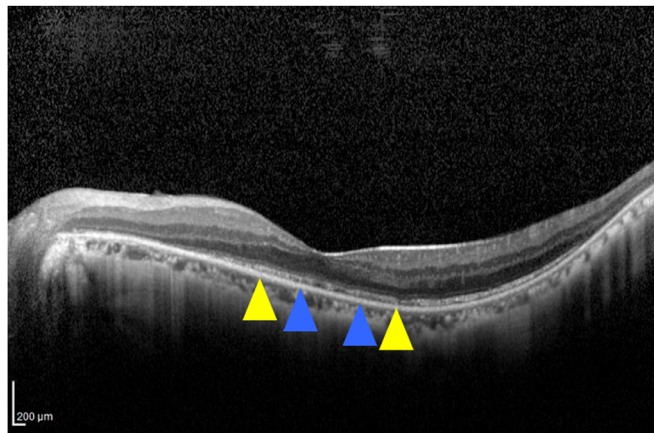

Figure 7. Representative OCT image in case with large prediction errors. There were 30 test points where the absolute prediction error was larger than 20 dB. The accompanied OCT image (horizontal scan, left eye) suggested that the ellipsoid zone was disrupted in the IN area and remained in the OUT areas. The region between blue and yellow arrows is ON area, whereas that between blue arrows is IN area. FAF, fluorescence autofluorescence; IN, inside the FAF ring; OCT, optical coherence tomography; ON, on the FAF ring.

suggested that VF sensitivity deteriorates when it is associated with the FAF measured with the Optos system in patients with RP.[17] We reported previously that the FAF ring diameter was more closely correlated with VF sensitivity than the ellipsoid zone disruption measured with OCT.[8] Using the currently proposed binarization method, it is possible to automatically identify the figure of FAF. This implies that it is useful to monitor the figure of FAF using the binarization method when assessing the progression of RP. The current results further suggested the possibility that the

HFA 10-2 test can be predicted using FAF, although further improvements are needed in the outer region for this to be used in clinical settings.

The current results suggested that the prediction was accurate in the central areas (IN and ON: see Figure 6 and Table 3. In contrast, the test points with the absolute prediction error > 20 dB were widely distributed across all 8 areas (from 2.2 to 4.2%). The disruption of the ellipsoid zone in the IN area usually occurs at the end stage of the disease. As suggested in Figure 7, the prediction accuracy of

the currently proposed method tended to be poor in eyes that the ellipsoid zone was disrupted in the IN area and remained in the OUT areas. In addition, significantly larger prediction error was observed with the deterioration of the visual functions (logMAR VA and TD value). This would suggest that it is needed to be careful when applying of the current model in such eyes. A future study would be needed to investigate whether a model using both FAF and ellipsoid zone result in the improvement of prediction accuracy, in such cases.

The current study has several limitations. First, the VF prediction using our binarization method is valid only for patients with RP with a complete FAF ring. Murakami et al. reported that the FAF ring was observed in 59% of patients with RP, whereas 18% of eyes had abnormal central FAF, and 24% of eyes had neither an FAF ring nor abnormal central FAF.[18] Second, analyses of VF and FAF were conducted in a cross-sectional manner. The comparison between the progressions of the VF and FAF ring over time would be of further interest. In addition, whereas the current study uses a much larger number of eyes than our previous study, confirmation may still be needed using a further larger dataset in the future.

In conclusion, VF sensitivity decreases in association with the FAF ring in patients with RP. It was possible to fairly accurately predict VF sensitivity using the FAF ring, particularly in the central area.

References

1. Hartong DT, Berson EL, Dryja TP. Retinitis pigmentosa. *Lancet.* 2006;368:1795–1809.

2. Abe K, Iijima H, Hirakawa H, Tsukahara Y, Toda Y. Visual acuity and 10 degrees automated static perimetry in eyes with retinitis pigmentosa. *Jpn J Ophthalmol.* 2002;46:581–585.

3. Swanson WH, Felius J, Birch DG. Effect of stimulus size on static visual fields in patients with retinitis pigmentosa. *Ophthalmology.* 2000;107:1950–1954.

4. von Rückmann A, Fitzke FW, Bird AC. Fundus autofluorescence in age-related macular disease imaged with a laser scanning ophthalmoscope. *Invest Ophthalmol Vis Sci.* 1997;38:478–486.

5. Nam KT, Yun CM, Kim JT, et al. Central serous chorioretinopathy fundus autofluorescence comparison with two different confocal scanning laser ophthalmoscopes. *Graefes Arch Clin Exp Ophthalmol.* 2015;253:2121–2127.

6. von Rückmann A, Fitzke FW, Bird AC. Distribution of pigment epithelium autofluorescence in retinal disease state recorded in vivo and its change over time. *Graefes Arch Clin Exp Ophthalmol.* 1999;237:1–9.

7. Robson AG, Egan CA, Luong VA, Bird AC, Holder GE, Fitzke FW. Comparison of fundus autofluorescence with photopic and scotopic fine-matrix mapping in patients with retinitis pigmentosa and normal visual acuity. *Invest Ophthalmol Vis Sci.* 2004;45:4119–4125.

8. Lee J, Asano S, Inoue T, et al. Investigating the usefulness of fundus autofluorescence in retinitis pigmentosa. *Ophthalmol Retina.* 2018;2:1062–1070.

9. Hashimoto Y, Inoue T, Ono T, et al. A novel method for the objective identification of hyperautofluorescent ring in retinitis pigmentosa using binarization processing. *Transl Vis Sci Technol.* 2019;8:20.

10. Bengtsson B, Heijl A. False-negative responses in glaucoma perimetry: indicators of patient performance or test reliability? *Invest Ophthalmol Vis Sci.* 2000;41:2201–2204.

11. Smith RT, Koniarek JP, Chan J, Nagasaki T, Sparrow JR, Langton K. Autofluorescence characteristics of normal foveas and reconstruction of foveal autofluorescence from limited data subsets. *Invest Ophthalmol Vis Sci.* 2005;46:2940–2946.

12. Kellner U, Kellner S, Weber BHF, Fiebig B, Weinitz S, Ruether K. Lipofuscin- and melanin-related fundus autofluorescence visualize different retinal pigment epithelial alterations in patients with retinitis pigmentosa. *Eye.* 2009;23:1349–1359.

13. Baayen RH, Davidson DJ, Bates DM. Mixed-effects modeling with crossed random effects for subjects and items. *J Mem Lang.* 2008;59:390–412.

14. Bates D, Mächler M, Bolker B, Walker S. Fitting linear mixed-effects models using lme4. *J Stat Softw.* 2015;67:1406.

15. Asaoka R. The relationship between visual acuity and central visual field sensitivity in advanced glaucoma. *Br J Ophthalmol.* 2013;97:1355–1356

16. Sayo A, Ueno S, Kominami T, et al. Significant relationship of visual field sensitivity in central 10° to thickness of retinal layers in retinitis pigmentosa. *Invest Ophthalmol Vis Sci.* 2018;59:3469–3475.

17. Oishi A, Ogino K, Makiyama Y, Nakagawa S, Kurimoto M, Yoshimura N. Wide-field fundus autofluorescence imaging of retinitis pigmentosa. *Ophthalmology.* 2013;120:1827–1834.

18. Murakami T, Akimoto M, Ooto S, et al. Association between abnormal autofluorescence and photoreceptor disorganization in retinitis pigmentosa. *Am J Ophthalmol.* 2008;145:687–694.